



# Synthesis and structural characterization of new ladder-like organostannoxanes derived from carboxylic acid derivatives: $[C_5H_4(p-CO_2)]_2[Bu_2Sn]_4(\mu_3-O)_2(\mu_2-OH)_2$ , $[Ph_2CHCO_2]_2[Bu_2Sn]_4(\mu_3-O)_2$ , and $[(p-NH_2)-C_6H_4-CO_2]_2[Bu_2Sn]_4(\mu_3-O)_2(\mu_2-OH)_2$

Tidiane Diop, Mouhamadou Birame Diop, Cheikh Abdoul Khadir Diop, Aminata Diasse-Sarr, Mamadou Sidibe, Florina Dumitru, Arie van Der Lee

## ► To cite this version:

Tidiane Diop, Mouhamadou Birame Diop, Cheikh Abdoul Khadir Diop, Aminata Diasse-Sarr, Mamadou Sidibe, et al.. Synthesis and structural characterization of new ladder-like organostannoxanes derived from carboxylic acid derivatives:  $[C_5H_4(p-CO_2)]_2[Bu_2Sn]_4(\mu_3-O)_2(\mu_2-OH)_2$ ,  $[Ph_2CHCO_2]_2[Bu_2Sn]_4(\mu_3-O)_2$ , and  $[(p-NH_2)-C_6H_4-CO_2]_2[Bu_2Sn]_4(\mu_3-O)_2(\mu_2-OH)_2$ . Main Group Metal Chemistry, 2022, 45 (1), pp.35-43. 10.1515/mgmc-2022-0008 . hal-03666480

HAL Id: hal-03666480

<https://hal.science/hal-03666480>

Submitted on 6 Oct 2023

**HAL** is a multi-disciplinary open access archive for the deposit and dissemination of scientific research documents, whether they are published or not. The documents may come from teaching and research institutions in France or abroad, or from public or private research centers.

L'archive ouverte pluridisciplinaire **HAL**, est destinée au dépôt et à la diffusion de documents scientifiques de niveau recherche, publiés ou non, émanant des établissements d'enseignement et de recherche français ou étrangers, des laboratoires publics ou privés.

## Research Article

Tidiane Diop\*, Mouhamadou Birame Diop, Cheikh Abdoul Khadir Diop, Aminata Diasse-Sarr, Mamadou Sidibe, Florina Dumitru, and Arie van der Lee

# Synthesis and structural characterization of new ladder-like organostannoxanes derived from carboxylic acid derivatives:

$[C_5H_4N(p-CO_2)]_2[Bu_2Sn]_4(\mu_3-O)_2(\mu_2-OH)_2$ ,  
 $[Ph_2CHCO_2]_4[Bu_2Sn]_4(\mu_3-O)_2$ , and  
 $[(p-NH_2)-C_6H_4-CO_2]_2[Bu_2Sn]_4(\mu_3-O)_2(\mu_2-OH)_2$

<https://doi.org/10.1515/mgmc-2022-0008>

received March 01, 2021; accepted March 05, 2022

**Abstract:** Three types of ladder-like organostannoxanes,  $[C_5H_4N(p-CO_2)]_2[Bu_2Sn]_4(\mu_3-O)_2(\mu_2-OH)_2$  (**1**),  $[Ph_2CHCO_2]_4[Bu_2Sn]_4(\mu_3-O)_2$  (**2**), and  $[(p-NH_2)-C_6H_4-CO_2]_2[Bu_2Sn]_4(\mu_3-O)_2(\mu_2-OH)_2$  (**3**), have been synthesized and characterized using elemental analyses, Fourier-transform infrared spectroscopy, nuclear magnetic resonance ( $^1H$ ,  $^{13}C$ ) experiments, and, for **1** and **2**, single-crystal X-ray diffraction analysis. X-Ray diffraction discloses that complexes adopt tetranuclear tin(IV) ladder-like structures containing two (**1**) or four (**2**) deprotonated ligands. The essential difference between their molecular structures is that in **2** there are four carboxylate ligands, while in **1** and **3** there are two. The crystal structure of **1** reveals them to be a tetranuclear structure containing a three-rung-staircase  $Sn_4O_4$  core. The  $Sn_4O_4$  cluster consists of a ladder of four  $Sn_2O_2$  units. For **2**, the structure is a tetranuclear centrosymmetric dimer of an oxoditin unit having a central four-member ring. In this complex, the

central  $Sn_2O_2$  core is fused with two four-member and two six-member rings. In the structures, there are two types of tin ions arranged in distorted trigonal bipyramidal geometry or octahedron geometry. A series of O–H···N, C–H···O, and C–H···π intermolecular hydrogen bonds in these complexes play an important function in the supramolecular, or two-dimensional network structures are formed by these interactions.

**Keywords:** diphenylacetate, pyridine-4-carboxylate, 4-aminobenzenecarboxylate, ladder and organostannoxanes

## 1 Introduction

During the past few decades, research on the synthesis and characterization of coordination polymers has intrigued scientists not only for their fascinating structures but also for their potential applications (Gielen et al., 2005; Kemmer et al., 2000; Willem et al., 1997). It has become apparent that coordination polymers may be prepared by the appropriate selection of metal and multi-functional ligands (Chandrasekhar et al., 2002, 2005; Diop et al., 2021). Among these materials, organotin(IV) carboxylate complexes have been actively investigated by a large number of researchers due to their significant reduction in tumor growth rates (Vieira et al., 2010), interesting topologies, and various structural types including monomers, dimers, tetramers, oligomeric ladders, and hexameric drums (Arjmand et al., 2014; Banti et al., 2019). The organostannoxanes have received special attentions, particularly in view of their immense structural diversity. Several products, such as ladders (Wen et al., 2018; García-Zarracino

\* Corresponding author: Tidiane Diop, Laboratoire de Chimie Minérale et Analytique, Département de Chimie, Faculté des Sciences et Techniques, Université Cheikh Anta Diop, Dakar, Sénégal, e-mail: tidiane3.diop@ucad.edu.sn

Mouhamadou Birame Diop, Cheikh Abdoul Khadir Diop,

Aminata Diasse-Sarr, Mamadou Sidibe: Laboratoire de Chimie Minérale et Analytique, Département de Chimie, Faculté des Sciences et Techniques, Université Cheikh Anta Diop, Dakar, Sénégal

Florina Dumitru: Politehnica University of Bucharest, Electrochemistry, Physical and Inorganic Chemistry Department, Polizu 1, RO-011061, Bucharest, Romania

Arie van der Lee: Institut Européen des Membranes, Université de Montpellier II, 34000 Montpellier, France

et al., 2009), cubes (Cavka et al., 2008), hexameric (Baul et al., 2017), and polymeric drums (Ma et al., 2003), have been isolated. Ladder-shaped tetranuclear organotin compounds (Wang et al., 2013) have also been isolated. Tetranuclear crystal structures  $[(n\text{-Bu}_2\text{Sn})_4(\text{O})_2(\text{OH})_2(\text{O}_3\text{SC}_6\text{H}_4\text{-NH}_2\text{-}4)_2]$  (Wen et al., 2018),  $[(\text{Me}_2\text{Sn})_4(\text{O})_2(\text{OH})_2(\text{O}_3\text{SC}_6\text{H}_4\text{-NH}_2\text{-}4)_2]$  (Wen et al., 2018), and  $[(n\text{-Bu}_2\text{Sn})_4(\mu_3\text{-O})_2(\mu_2\text{-OCH}_3)_2(\text{O}_2\text{CC}_6\text{H}_4\text{-SO}_2\text{NH}_2\text{-}4)_2]$  (Wang et al., 2019) with the ladder as structural motif were previously described in the literature. Many butyl-stannoxyanes were prepared using carboxylate ligands (Baul et al., 2017; Shankar and Dubey, 2020; Valcarcel et al., 2012; Wang et al., 2019). These molecular structures of compounds display hexameric  $\text{Sn}_6\text{O}_6$  clusters with drum-like or tetrameric structures revealing  $\text{Sn}_4\text{O}_2$  cores with ladder-type structural motifs. In our previous work, we reported a series of butyl-stannoxyanes carboxylate complexes using carboxylic acid ligands such as pyridine-4-carboxylic acid, diphenylacetic acid, and 4-aminocarboxylic acid. The synthesis and structural characterization of three new organostannoxyanes are reported as follows:  $[\text{C}_5\text{H}_4\text{N}(p\text{-CO}_2)]_2[\text{Bu}_2\text{Sn}]_4(\mu_3\text{-O})_2(\mu_2\text{-OH})_2$  (**1**),  $[\text{Ph}_2\text{CHCO}_2]_2[\text{Bu}_2\text{Sn}]_4(\mu_3\text{-O})_2$  (**2**), and  $[(p\text{-NH}_2)\text{-C}_6\text{H}_4\text{-CO}_2]_2[\text{Bu}_2\text{Sn}]_4(\mu_3\text{-O})_2(\mu_2\text{-OH})_2$  (**3**).

## 2 Results

### 2.1 Crystallographic data and experimental details

Crystal data, data collection, and structure refinement details for the complex are summarized in Table 1.

## 3 Discussion

### 3.1 Reactions

The general chemical reactions in methanol are shown for complexes **1** and **3** Eq. (1) and for complex **2** Eq. (2):

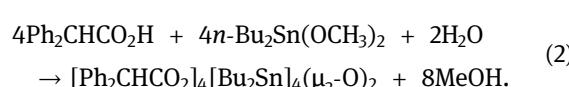
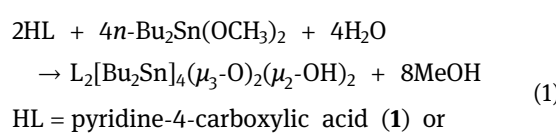


**Table 1:** Crystal data and structure refinement of **1** and **2**

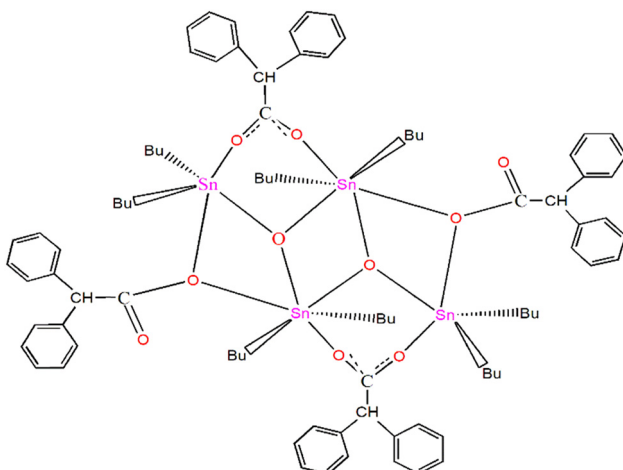
	<b>1</b>	<b>2</b>
Formula	$\text{C}_{44}\text{H}_{82}\text{N}_2\text{O}_8\text{Sn}_4$	$\text{C}_{88}\text{H}_{116}\text{O}_{10}\text{Sn}_4$
Moity	$\text{C}_{44}\text{H}_{82}\text{N}_2\text{O}_8\text{Sn}_4$	$\text{C}_{88}\text{H}_{116}\text{O}_{10}\text{Sn}_4$
T (K)	175	175
Spacegroup	$P2_1/n$	$P-1$
Crystal system	Monoclinic	Triclinic
a (Å)	13.0597(5)	15.6908(7)
b (Å)	12.2041(6)	15.7536(8)
c (Å)	17.0979(6)	19.4517(8)
$\alpha$ (°)	90	83.718(4)
$\beta$ (°)	96.017(4)	75.218(4)
$\gamma$ (°)	90	64.601(5)
V (Å <sup>3</sup> )	2710.09(19)	4199.7(4)
Z	2	2
$P$ (g cm <sup>-3</sup> )	1.522	1.430
$M_r$ (g mol <sup>-1</sup> )	1241.96	1808.65
$\mu$ (mm <sup>-1</sup> )	1.867	1.231
$R_{\text{int}}$	0.065	0.084
$\theta_{\text{max}}$ (°)	29.091	29.464
Resolution (Å)	0.79	0.82
$N_{\text{tot}}$ (measured)	18,164	52,524
$N_{\text{ref}}$ (unique)	6,381	19,770
$N_{\text{ref}}$ ( $I > 2\sigma(I)$ )	4,462	10,858
$N_{\text{ref}}$ (least-squares)	4,462	10,858
$N_{\text{par}}$	285	928
$\langle \sigma(I)/I \rangle$	0.0807	0.1165
$R_1$ ( $I > 2\sigma(I)$ )	0.0901	0.0689
$wR_2$ ( $I > 2\sigma(I)$ )	0.0390	0.0887
$R_1$ (all)	0.1325	0.1292
$wR_2$ (all)	0.0488	0.01682
GOF	1.4261	1.1410
$\Delta\rho$ (e Å <sup>-3</sup> )	-1.56/3.26	-1.70/3.72
Crystal size (mm)	0.12 × 0.15 × 0.20	0.22 × 0.25 × 0.30

After synthesis, the complexes are characterized by elemental analyses, Fourier-transform infrared spectroscopy and nuclear magnetic resonance (<sup>1</sup>H, <sup>13</sup>C) experiments, and, for **1** and **2**, single-crystal X-ray diffraction.

### 3.2 Spectroscopic studies

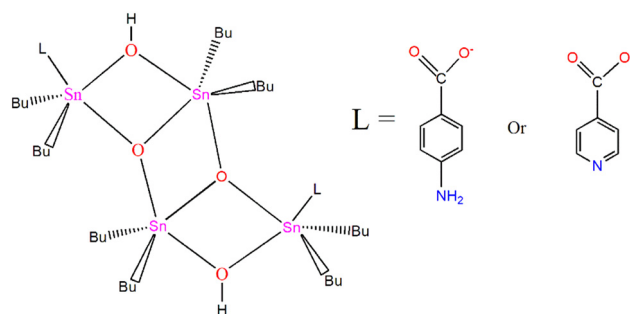
#### 3.2.1 FT-IR spectra

The explicit feature in the FTIR spectra is the absence of a broadband in the region 3,400–2,800 cm<sup>-1</sup>, which appears in the free ligands for the COOH group, indicating the removal of COOH protons and the formation of Sn–O bonds through this site (Li et al., 2010; Zhang et al., 2012). The strong absorption appearing at 444 (**1**), 436 (**2**), and 433 (**3**) cm<sup>-1</sup> is assigned to  $\nu(\text{Sn}-\text{O})$  (Xiao et al., 2013).



**Scheme 1:** Structures of  $[C_5H_4N(p-CO_2)]_2[Bu_2Sn]_4(\mu_3-O)_2(\mu_2-OH)_2$  (**1**) or  $[(p-NH_2)-C_6H_4-CO_2]_2[Bu_2Sn]_4(\mu_3-O)_2(\mu_2-OH)_2$  (**3**).

The intense absorption maximum in the  $623\text{--}630\text{ cm}^{-1}$  region is assigned to an Sn–O–Sn stretching vibration (Li et al., 2015). In the infrared spectra of this complex, the  $\Delta\nu(C(O)O)$  [ $\nu(C(O)O)_{\text{asym}} - \nu(C(O)O)_{\text{sym}}$ ] values are  $299\text{ cm}^{-1}$  for **1** and  $273\text{ cm}^{-1}$  for **3**, larger than  $200\text{ cm}^{-1}$ , which stands for the monodentate coordination mode of the carboxylate groups (Hanif et al., 2010), and this behavior is also consistent with the X-ray structure. The two  $\Delta\nu$  magnitudes ( $\nu_{\text{asymCOO}} - \nu_{\text{symCOO}}$ )  $254$  and  $143\text{ cm}^{-1}$  for (**2**) show that two distinct coordination modes for carboxylate ligands are present in the structure (Eng et al., 2007). One carboxylate fragment is symmetrically bridged between two Sn ions, and another carboxylate acts as a bis-monodentate ligand for Sn atoms (Scheme 2). The presence of a  $\nu_{\text{asymCOO}}$  band at  $617\text{ cm}^{-1}$  (**1**),  $615\text{ cm}^{-1}$  (**2**), and  $613\text{ cm}^{-1}$  (**3**) indicates a nonlinear  $SnBu_2$  residue (Nakamoto, 1997; Beckman et al., 2004) (Schemes 1 and 2). The conclusions drawn from the IR data are very much consistent with those of the X-ray crystallography studies.



**Scheme 2:** Structure of  $[Ph_2CHCO_2]_4[Bu_2Sn]_4(\mu_3-O)_2$  (**2**).

### 3.2.2 NMR spectra

The  $^1\text{H}$  and  $^{13}\text{C}$  NMR data of the complexes are given in the experimental part, and the observed resonances have been assigned based on the chemical shift values. In the  $^1\text{H}$  NMR spectra, the expected signals in the  $10\text{--}13\text{ ppm}$  region of the carboxylic acid hydrogens are not present in the complexes, indicating the replacement of the carboxylic acid protons with organotin(IV) moieties (Najafi et al., 2014; Xiao et al., 2013). The order of the  $^1\text{H}$  chemical shifts of the  $CH_n$  groups in the Sn–butyl substituents was found to be  $(\alpha, \beta) > (\gamma, \delta)$  for the  $Bu_2Sn$  complexes ( $SnCH_2(\alpha)CH_2(\beta)CH_2(\gamma)CH_3(\delta)$ ) (Pruchnik et al., 2013). Multiplet signals in the  $1.50\text{--}1.86$ ,  $1.25\text{--}1.43$ , and  $0.92\text{--}0.93\text{ ppm}$  ranges are attributed to  $(m, \alpha\text{-}CH_2, \beta\text{-}CH_2)$ ,  $(m, \gamma\text{-}CH_2)$ , and  $(t, \delta\text{-}CH_3)$ , respectively. The multiplet signals at  $8.12\text{--}6.77\text{ ppm}$  are assigned to aromatic protons. In the  $^{13}\text{C}$  NMR spectra of all the complexes, peaks at  $167.41$  (**1**),  $175.1$  (**2**), and  $179.34$  (**3**) ppm attributed to  $COO^-$  groups show a downfield shift of all the carbon resonances compared to the free carboxylates. These conclusions are consistent with those of the IR data and the X-ray crystal structures.

The structures for complexes **1**, **2**, and **3** are  $Sn_4O_4$  tetramers with either monodentate or bridging carboxylate ligands (Schemes 1 and 2).

### 3.3 Crystal structure of complex 1

A perspective view of the molecular structure of complex **1** is illustrated in Figures 1 and 2. Selected bond lengths ( $\text{\AA}$ ) and angles ( $^\circ$ ) are listed in Table 2. The structure consists of the hydroxide-bridged tetranuclear organostannoxane

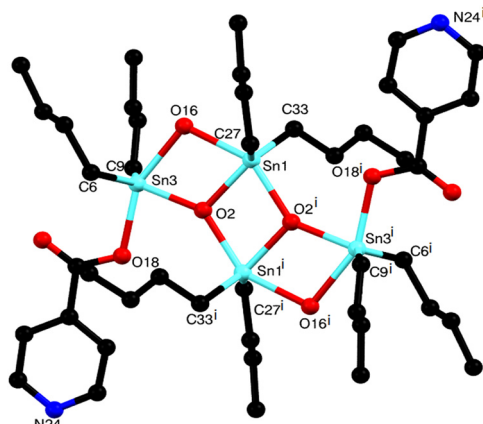


**Figure 1:** Tetranuclear structure of  $[C_5H_4N-(p-CO_2)]_2[Bu_2Sn]_4(\mu_3-O)_2(\mu_2-OH)_2$  (**1**).

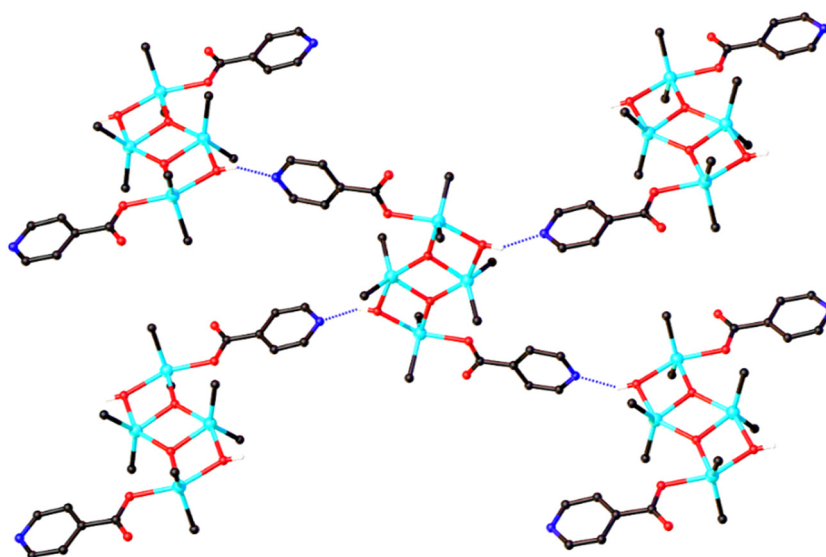


**Figure 2:** Crystal structure in an infinite chain of  $[C_5H_4N-(p-CO_2)]_2[Bu_2Sn]_4(\mu_3-O)_2(\mu_2-OH)_2$  (**1**) with O–H…N intermolecular hydrogen bonds. Only *Cipso* of the *n*-butyl groups are shown for clarity.

**Table 2:** Geometric parameters (Å and °) of complex **1**

Lengths (Å)	Angles (°)				
Sn1–O2i	2.128 (3)	O2i–Sn1–O2	74.51 (17)	Sn1i–O2–Sn3	143.67 (18)
Sn1–O2	2.062 (4)	O2i–Sn1–Sn3	108.55 (10)	Sn1–O2–Sn3	110.83 (15)
Sn1–O16	2.139 (4)	O2i–Sn1–O16	147.95 (14)	O2–Sn3–C6	112.9 (2)
Sn1–C27	2.106 (7)	O2–Sn1–O16	73.44 (14)	O2–Sn3–C9	112.2 (3)
Sn1–C33	2.139 (7)	O2i–Sn1–C27	95.6 (2)	C6–Sn3–C9	134.7 (3)
O2–Sn3	2.005 (4)	O2–Sn1–C27	115.2 (3)	O2–Sn3–O16	73.80 (15)
Sn3–C6	2.087 (7)	O16–Sn1–C27	98.3 (3)	C6–Sn3–O16	91.8 (2)
Sn3–C9	2.166 (8)	O2i–Sn1–C33	99.2 (2)	C9–Sn3–O16	96.3 (3)
Sn3–O16	2.173 (4)	O2–Sn1–C33	115.8 (3)	O2–Sn3–O18	80.31 (14)
Sn3–O18	2.176 (4)	O16–Sn1–C33	94.2 (3)	C6–Sn3–O18	99.1 (2)
		C27–Sn1–C33	129.0 (3)	C9–Sn3–O18	92.6 (2)
		Sn1i–O2–Sn1	105.49 (17)	O16–Sn3–O18	154.09 (16)

Symmetry code: (i)  $-x, -y, -z + 1$ .

ladder and two deprotonated pyridine-4-carboxylic ligands. The complex adopts tetranuclear tin(IV) ladder-like structure containing two deprotonated ligands linked by three alternate  $Sn_2O_2$  four-membered rings. As is shown in **1**, the molecular structure is a centrosymmetric ladder-like structure consisting of the  $Sn_4(\mu_3-O)_2(\mu_2-OH)_2$  group and two deprotonated ligands. As is the case for other usual tetrameric organostannoxanes (Li *et al.*, 2015), the structure is based on a centrosymmetric  $Sn_2O_2$  unit connected to a pair of exocyclic Sn atoms via bridging  $\mu_3$ -O atoms. Triply bridged  $\mu_3$ -O atoms, which share their electrons with three tin(IV) centers, have distorted tetrahedral configurations. All the Sn atoms are five-coordinated, showing a trigonal bipyramidal configuration in two different chemical environments:

$SnBu_2O_2(OH)$  and  $SnBu_2O(OH)[C_5H_4N(p-CO_2)]$ . For Sn(1) atom (exocyclic), the basal plane is defined by C(33), C(27), and O(2), and the axial sites occupied by the O(2i) and O(16) atoms, which form an angle of 147.95 (14)°, deviating from a linear arrangement. The carboxylate moiety  $COO^-$  of the ligand is bonded as a monodentate mode with Sn(3)–O(18) (2.176 Å) way as depicted in Table 2. These bond lengths are in accordance with those of the reported di-*n*-butyltin(IV) carboxylates (Xiao *et al.*, 2013; Zhu *et al.*, 2011).

Intermolecular O–H…N hydrogen bonds, involving the bridging hydroxy group and the N atom of the ligand, connect the discrete units into a two-dimensional (2D) network (Figure 2). For the O–H…N intermolecular interactions and C–H…O intramolecular interactions (Figure 3),

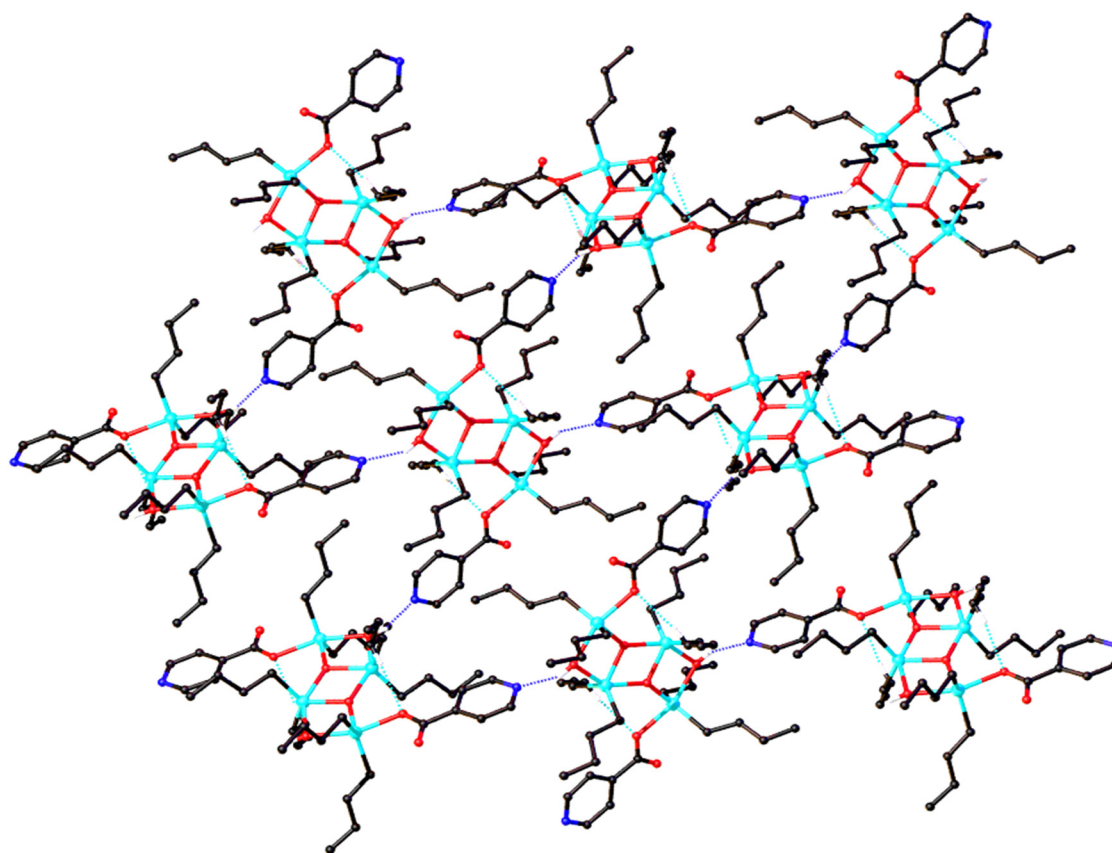


**Figure 3:** Crystal structure in infinite chain of  $[C_5H_4N-(p-CO_2)]_2[Bu_2Sn]_4(\mu_3-O)_2(\mu_2-OH)_2$  (**1**) with intermolecular hydrogen bonds O-H···N (color code: blue) and intramolecular hydrogen bonds C-H···O (color code: greenish). Only *C<sub>i</sub>psos* of the *n*-butyl groups are shown for clarity.

**Table 3:** Hydrogen-bond geometry (Å and °) of complex **1**

D-H···A	D-H	H···A	D···A	D-H···A
O16-H161···N24 <sup>ii</sup>	0.82 (2)	2.06 (4)	2.810 (14)	153 (8)
C34-H341···O18i	0.98	2.59	3.440 (14)	145

Symmetry codes: (i)  $-x, -y, -z + 1$ ; (ii)  $x + 1/2, -y - 1/2, z - 1/2$ .

the H(161)···N(24ii) and H(341)···O(18i) distances are 2.06(4) and 2.59 Å, respectively. The O(16)–H(161)···N(24ii) and C(34)–H(341)···O(18i) angles are 153(8) and 145° (Table 3). The hydrogen-bond geometry is close to the values reported for  $[(n\text{-}Bu_2Sn)_2(\mu_3\text{-}O)(\mu\text{-}OH)L]_2$  (Li et al., 2015). The crystallographic study confirms the spectroscopic conclusions.

### 3.4 Crystal structure of complex 2

The asymmetric unit features linkage of neighboring monomers by hydrogen-bond interactions [C–H···O and C–H···π], giving rise to the formation of organotin(IV) aggregate (Figure 4). Selected bond lengths (Å) and angles (°) are

listed in Table 4. The conformations of the two independent molecules are almost the same, except for small differences in angles and bond lengths. The crystal structure is very similar to that reported by Zhang et al. (2012). The structure is a tetranuclear centrosymmetric dimer of an oxoditin(IV) unit having a central four-member ring composed of  $Sn(3)\text{-}O(2)\text{-}Sn(3^i)\text{-}O(2^i)$ . In this complex, the central  $Sn_2O_2$  core is fused with two four-member and two six-member rings. The four-member rings, that is,  $[Sn_2O_2]$ , i.e.,  $O(28)\text{-}Sn(1)\text{-}O(2)\text{-}Sn(3^i)$  and  $O(28^i)\text{-}Sn(1^i)\text{-}O(2^i)\text{-}Sn(3)$ , are due to the bridging of the monodentate ligand through O atoms,  $O(28)\text{-}Sn(1)$ , and  $O(28^i)\text{-}Sn(1^i)$ , respectively. Two six-member rings  $[Sn_2O_3C]$ ; i.e.,  $Sn(1)\text{-}O(6)\text{-}C(5)\text{-}O(4)\text{-}Sn(3)\text{-}O(2)$ ,  $Sn(1^i)\text{-}O(6^i)\text{-}C(5^i)\text{-}O(4^i)\text{-}Sn(3^i)\text{-}O(2^i)$ ] also overlap central  $Sn_2O_2$ . As is the case for other usual tetrameric organostannoxane (Li et al., 2015), the structure is based on a centrosymmetric  $Sn_2O_2$  unit connected to a pair of exocyclic Sn atoms via bridging  $\mu_3\text{-}O$  atoms. There are two distinct carboxylate ligands in the structure. The first carboxylate, defined by the O(4) and O(6) atoms, symmetrically bridges the exocyclic  $Sn(3)$  and endocyclic  $Sn(1)$  atoms. The second carboxylate is a bis-monodentate

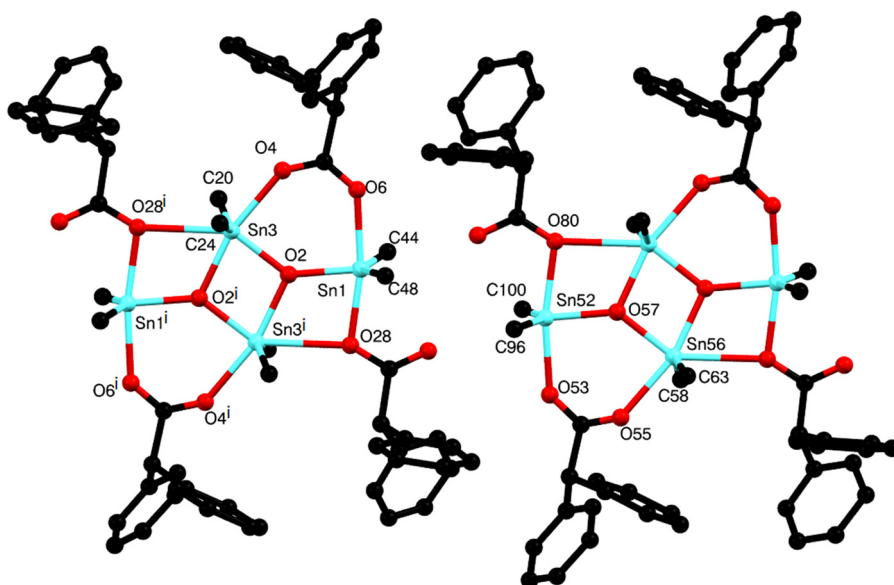


**Figure 4:** The ladder structure of aggregate complex **2** (hydrogen atoms bonded to carbon atoms are omitted, and only the  $\alpha$ -carbon of the butyl groups has been drawn for clarity).

**Table 4:** Geometric parameters ( $\text{\AA}$  and  $^\circ$ ) of complex **2**

Lengths ( $\text{\AA}$ )	Angles ( $^\circ$ )				
Sn1–O2	2.044 (8)	O2–Sn1–O6	91.7 (3)	O28i–Sn3–O4	127.7 (3)
Sn1–O6	2.276 (9)	O2–Sn1–O28	78.3 (3)	O2i–Sn3–C20	100.0 (4)
Sn1–O28	2.198 (8)	O6–Sn1–O28	169.9 (3)	O2–Sn3–C20	105.2 (4)
Sn1–C44	2.143 (12)	O2–Sn1–C44	112.0 (4)	O28i–Sn3–C20	79.4 (4)
Sn1–C48	2.128 (13)	O6–Sn1–C44	84.4 (4)	O2i–Sn3–C24	99.6 (4)
O2–Sn3i	2.143 (7)	O28–Sn1–C44	98.2 (4)	O2–Sn3–C24	108.8 (4)
O2–Sn3	2.061 (8)	O2–Sn1–C48	108.4 (4)	O28i–Sn3–C24	80.8 (4)
Sn3–O28i	2.669 (9)	O6–Sn1–C48	89.2 (4)	O4–Sn3–C20	85.3 (5)
Sn3–O4	2.262 (9)	O28–Sn1–C48	95.0 (4)	O4–Sn3–C24	83.2 (5)
Sn3–C20	2.137 (13)	C44–Sn1–C48	139.2 (5)	C20–Sn3–C24	143.7 (5)
Sn3–C24	2.117 (12)	Sn3i–O2–Sn1	119.4 (3)	Sn3–O4–C5	138.9 (8)
Sn52–O53	2.218 (8)	Sn3i–O2–Sn3	103.0 (3)	O2–Sn3–O4	88.6 (3)
Sn52–O57	2.047 (8)	Sn1–O2–Sn3	137.6 (4)	O2i–Sn3–O4	165.5 (3)
Sn52–O80	2.203 (7)	O2i–Sn3–Sn3i	37.6 (2)	O2i–Sn3–O28i	66.7 (3)
Sn52–C96	2.119 (14)	O2i–Sn3–O2	77.0 (3)		
Sn52–C100	2.113 (14)	O2–Sn3–O28i	143.6 (3)		
O55–Sn56,	2.298 (10)				
Sn56–O57ii	2.126 (8)				

Symmetry codes: (i)  $-x + 1, -y + 1, -z$ ; (ii)  $-x + 1, -y + 2, -z + 1$ .

coordinating ligand to the exocyclic Sn(3) and endocyclic Sn() via  $\mu$ -O(28) atom (Figure 4). The endocyclic Sn(3) exists in a distorted octahedron geometry with the four O atoms [O(4), O(6), O(2), and O(28i)] defining the basal plan. The axial position is occupied by C(20) and C(24) which form an angle C(20)–Sn(3)–C(24) of 143.7 (5) (Table 4). The exocyclic Sn(1) atoms are five coordinated and show distorted trigonal bipyramidal geometry with the

basal plan defined by the  $\mu_3$ -O(2) atom, the C(48) and C(44) atoms. The axial angle of O(6)–Sn(1)–O(28i) is 169.9°(3).

Intermolecular C–H...O and C–H... $\pi$  hydrogen bonds are recognized in complex **2**, which link the molecular structure into 2D network. For the C–H...O interactions, the distances [H...O, in the 2.35–2.60  $\text{\AA}$  ranges] and [H... $\pi$ , in the 2.40–2.60  $\text{\AA}$  ranges] (Table 5) are all close to the values reported by Li *et al.* (2015).

**Table 5:** Hydrogen-bond geometry (Å and °) of complex 2

D–H…A	D–H	H…A	D…A	D–H…A
C12–H121…C61 <sup>ii</sup>	0.93	2.40	3.11 (3)	134
C19–H191…O4	0.93	2.47	3.09 (3)	124
C37–H371…O30	0.93	2.44	3.05 (3)	124
C44–H442…O82 <sup>iii</sup>	0.97	2.60	3.37 (3)	136
C79–H791…O55	0.93	2.35	3.00 (3)	127
C89–H891…O82	0.93	2.43	3.05 (3)	124
C96–H962…O30 <sup>iv</sup>	0.97	2.56	3.26 (3)	129
C103–H1031…C62	1.05	2.60	3.54 (3)	149

Symmetry codes: (ii)  $-x + 1, -y + 2, -z + 1$ ; (iii)  $x, y - 1, z$ ; (iv)  $x, y + 1, z$ .

## 4 Conclusion

Carboxylate clusters with a  $\text{Sn}_4\text{O}_4$  ladder framework and a centrosymmetric  $\text{Sn}_2\text{O}_2$  dimer as structural motifs have been successfully synthesized and characterized by elemental analyses, FTIR, NMR spectra, and X-ray single-crystal diffraction. These three ladder-shaped organostannoxane compounds reveal rich supramolecular structures as a result of intermolecular hydrogen bonds. In the crystalline state, the center Sn(IV) atoms of complexes **1** and **2** adopt five-, six-coordination mode, display trigonal bipyramidal and octahedron geometry, and reveal rich supramolecular structures by intermolecular hydrogen-bonding interactions. The carboxylates are either bidentate bridging or monodentate.

## Experimental

### Synthesis of $[\text{C}_5\text{H}_4\text{N}(\text{p}-\text{CO}_2)]_2[\text{Bu}_2\text{Sn}]_4(\mu_3\text{-O})_2(\mu_2\text{-OH})_2$ (**1**)

A methanolic solution containing 0.20 g (0.16 mmol) of pyridine-4-carboxylic acid,  $\text{C}_5\text{H}_4\text{N}-(\text{p}-\text{CO}_2\text{H})$ , was added to a methanolic solution which contains 0.1 g (0.32 mmol) of di(*n*-butyl)dimethoxystannane, *n*-Bu<sub>2</sub>Sn(OCH<sub>3</sub>)<sub>2</sub>. The mixture was stirred at room temperature for more than 4 h. After the slow evaporation of the solvent, a white crystal was collected and characterized as  $[\text{C}_5\text{H}_4\text{N}(\text{p}-\text{CO}_2)]_2[\text{Bu}_2\text{Sn}]_4(\mu_3\text{-O})_2(\mu_2\text{-OH})_2$ , yield: 60%; IR (ATR, cm<sup>-1</sup>): 1,643  $\nu(\text{OCO})_{\text{asym}}$ , 1,408  $\nu(\text{OCO})_{\text{sym}}$ , 299  $\Delta\nu$ , 1,601/1,557  $\nu\text{C}=\text{C/C=N}$ , 709 vaSnC<sub>2</sub>, 625 vs(Sn–O–Sn), 617 vsSnC<sub>2</sub>, 444  $\nu\text{Sn-O}$ . <sup>1</sup>H NMR (CDCl<sub>3</sub>, ppm): SnCH<sub>2</sub>CH<sub>2</sub>CH<sub>2</sub>CH<sub>3</sub>,  $\delta = 1.78\text{--}1.60$  (m, CH<sub>2</sub>–CH<sub>2</sub>); 1.43–1.25 (m, CH<sub>2</sub>); 0.93 (t, CH<sub>3</sub>). Ligand, 7.5 (m, aromatic protons), 6.87 (m, aromatic protons).

protons). <sup>13</sup>C NMR (CDCl<sub>3</sub>, ppm): SnCH<sub>2</sub>CH<sub>2</sub>CH<sub>2</sub>CH<sub>3</sub>, 31.60[Sn–CH<sub>2</sub>], 28.00[CH<sub>2</sub>], 25.31[CH<sub>2</sub>], 15.23[CH<sub>3</sub>]. Carbons of the ligands, 167.41 (CO<sub>2</sub>); 130.6, 128.61, 127.83 (aromatic carbons). Anal. calc. for: C<sub>46</sub>H<sub>86</sub>N<sub>2</sub>O<sub>8</sub>Sn<sub>4</sub> (1,241.91): C, 42.53%; H, 6.50%; N, 2.20%. Found: C 42.55%; H, 6.65%; N, 2.26%.

### Synthesis of $[\text{Ph}_2\text{CHCO}_2]_4[\text{Bu}_2\text{Sn}]_4(\mu_3\text{-O})_2$ (**2**)

The preparation of  $[\text{Ph}_2\text{CHCO}_2]_4[\text{Bu}_2\text{Sn}]_4(\mu_3\text{-O})_2$  is similar to that of complex **1** with diphenylacetic acid 0.20 g (0.11 mmol) as carboxylate ligand 1:1 molar ratio. The mixture was stirred for around 3 h at room temperature and upon slow solvent evaporation, white-colored, prismatic crystals suitable for X-ray diffraction analysis have grown. Yield: 64%; IR (ATR, cm<sup>-1</sup>): 1,550  $\nu(\text{OCO})_{\text{asym}}$ , 1,386/1,497  $\nu(\text{OCO})_{\text{sym}}$ , 254/143  $\Delta\nu$ , 1,571  $\nu\text{C}=\text{C}$ , 709 vaSnC<sub>2</sub>, 623 vs(Sn–O–Sn), 615 vsSnC<sub>2</sub>, 436  $\nu\text{Sn-O}$ . <sup>1</sup>H NMR (CDCl<sub>3</sub>, ppm): SnCH<sub>2</sub>CH<sub>2</sub>CH<sub>2</sub>CH<sub>3</sub>,  $\delta = 1.86$  (m, CH<sub>2</sub>–CH<sub>2</sub>); 1.59 (m, CH<sub>2</sub>); 0.92 (t, CH<sub>3</sub>). Ligand, 7.8 (s, CH), 7.5 (m, aromatic protons), 6.60 (m, aromatic protons). <sup>13</sup>C NMR (CDCl<sub>3</sub>, ppm): SnCH<sub>2</sub>CH<sub>2</sub>CH<sub>2</sub>CH<sub>3</sub>, 28.7[Sn–CH<sub>2</sub>], 26.5[CH<sub>2</sub>], 27.7[CH<sub>2</sub>], 13.5[CH<sub>3</sub>]. Carbons of the ligands, 175.1 (CO<sub>2</sub>); 153.1 (CH); 128.64, 127.56, 127.17 (aromatic carbons). Anal. calc. for: C<sub>88</sub>H<sub>116</sub>O<sub>10</sub>Sn<sub>4</sub> (1,808.7): C, 58.75%; H, 6.44%. Found: C, 58.44%; H, 6.44%.

### Synthesis of $[(p\text{-NH}_2)\text{-C}_6\text{H}_4\text{-CO}_2]_2[\text{Bu}_2\text{Sn}]_4(\mu_3\text{-O})_2(\mu_2\text{-OH})_2$ (**3**)

The preparation of  $[(p\text{-NH}_2)\text{-C}_6\text{H}_4\text{-CO}_2]_2[\text{Bu}_2\text{Sn}]_4(\mu_3\text{-O})_2(\mu_2\text{-OH})_2$  (**3**) followed that of complex **1**, with (p-NH<sub>2</sub>)-C<sub>6</sub>H<sub>4</sub>-CO<sub>2</sub> 0.21 g (0.16 mmol) used as carboxylic acid in 1:2 molar ratio. The mixture was stirred for around 3 h at room temperature, and upon slow solvent evaporation, a white powder resulted. Yield: 53%; IR (ATR, cm<sup>-1</sup>): 1,623  $\nu(\text{OCO})_{\text{asym}}$ , 1,350  $\nu(\text{OCO})_{\text{sym}}$ , 273  $\Delta\nu$ , 1,588  $\nu\text{C}=\text{C/C=N}$ , 630 vs(Sn–O–Sn), 701 vaSnC<sub>2</sub>, 613 vsSnC<sub>2</sub>, 433  $\nu\text{Sn-O}$ . <sup>1</sup>H NMR (CDCl<sub>3</sub>, ppm): SnCH<sub>2</sub>CH<sub>2</sub>CH<sub>2</sub>CH<sub>3</sub>,  $\delta = 1.70\text{--}1.65$  (m, CH<sub>2</sub>–CH<sub>2</sub>); 1.35–1.20 (m, CH<sub>2</sub>); 0.95 (t, CH<sub>3</sub>). Ligand, 7.5 (m, aromatic protons); 6.87 (m, aromatic protons). <sup>13</sup>C NMR (CDCl<sub>3</sub>, ppm): SnCH<sub>2</sub>CH<sub>2</sub>CH<sub>2</sub>CH<sub>3</sub>, 31.46[Sn–CH<sub>2</sub>], 29.32[CH<sub>2</sub>], 26.36[CH<sub>2</sub>], 14.10[CH<sub>3</sub>]. Carbons of the ligands, 179.34 (CO<sub>2</sub>); 128.64, 127.56, 127.17 (aromatic carbons). Anal. calc. for: C<sub>46</sub>H<sub>86</sub>N<sub>2</sub>O<sub>8</sub>Sn<sub>4</sub> (1,270.02): C, 43.50%; H, 6.83%; N, 2.21%. Found: C, 42.75%; H, 6.53%; N, 2.40%.

## Materials and methods

### Synthesis and spectroscopic materials

Pyridine-4-carboxylic acid, *p*-aminobenzoic acid, diphenylacetic acid, *n*-Bu<sub>2</sub>Sn(OCH<sub>3</sub>)<sub>2</sub>, and solvents were obtained from Aldrich and were used without further purification. Elemental analysis (C, H, and N) was performed using a Perkin–Elmer model 2400 CHN elemental analyzer. IR spectra in the range 4,000–400 cm<sup>−1</sup> were recorded using FT-IR spectrophotometer *Nicolet 710 TF-IR* operated by the OMNIC software. <sup>1</sup>H and <sup>13</sup>C NMR spectra were recorded in CDCl<sub>3</sub> solution on BRUKER DPX-300 and BRUKER AVANCE II 400 spectrometers with *Topspin 2.1* as software. The spectra were acquired at room temperature (298 K). <sup>13</sup>C NMR spectra are broadband-proton-decoupled. The chemical shifts were reported in ppm with respect to the references and were stated relative to external tetramethylsilane for <sup>1</sup>H and <sup>13</sup>C NMR.

### X-Ray crystallography

The X-ray crystallographic data were collected using a Rigaku Oxford-Diffraction Gemini-S diffractometer. All data were collected with graphite monochromated Mo-K $\alpha$  radiation ( $\lambda = 0.71073 \text{ \AA}$ ) at 175 K. *CrysAlis PRO* (released on August 13, 2014, CrysAlis171.NET) (compiled on August 13, 2014, 18:06:01); cell refinement: *CrysAlis PRO*, Agilent Technologies, Version 1.171.37.35 (released on August 13, 2014, CrysAlis171.NET) (compiled on August 13, 2014, 18:06:01); data reduction: *CrysAlis PRO*, Agilent Technologies, Version 1.171.37.35 (released on August 18, 2014, CrysAlis171.NET) (compiled on August 13, 2014, 18:06:01); program(s) used to solve structure: Superflip (Palatinus and Chapuis, 2007); program(s) used to refine structure: *CRYSTALS* (Betteridge *et al.*, 2003); molecular graphics: *CAMERON* (Watkin *et al.*, 1996). Programs used for the representation of the molecular and crystal structures were Olex2 (Dolomanov *et al.*, 2009) and Mercury (Macrae *et al.*, 2008).

### Accession codes

CCDC 2053062 (**1**) and 2053063 (**2**) contain the supplementary crystallographic data for this article. Copies can be obtained free of charge from the Cambridge Crystallographic Data Centre (CCDC), 12 Union Road, Cambridge CB2 1EZ, UK

(fax: int. Code +44 1223 336 033; e-mail: deposit@ccdc.cam.ac.uk or http://www.ccdc.cam.ac.uk).

**Acknowledgments:** The authors gratefully acknowledge the Cheikh Anta Diop University, Dakar (Senegal), the University of Montpellier, Montpellier (France), for equipment and financial support.

**Funding information:** Authors state that no funding is involved.

**Author contributions:** Tidiane Diop: methodology, writing – original draft, writing – original draft preparation; Mouhamadou Birame Diop: refinement of structures; Cheikh Abdoul Khadir Diop: conceptualization, writing – original draft; Aminata Diasse-Sarr: conceptualization project administration; Mamadou Sidibe: conceptualization, project administration; Florina Dumitru: writing – original draft, supervision, Arie van der Lee: writing – original draft, crystal analysis, supervision.

**Conflict of interest:** The authors state no conflict of interest.

## References

- Arjmand F., Parveen S., Tabassum S., Pettinari C., Organotin anti-tumor compounds: their present status in drug development and future perspectives. *Inorg. Chim. Acta*, 2014, 423, 26–37.
- Banti C.N., Hadjikakou S.K., Sismanoglu T., Hadjiliadis N., Anti-proliferative and antitumor activity of organotin(IV) compounds. An overview of the last decade and future perspectives. *J. Inorg. Biochem.*, 2019, 194, 114–152.
- Baul T.S.B., Dutta D., Duthie A., Guedes da Silva M.F.C., Perceptive variation of carboxylate ligand and probing the influence of substitution pattern on the structure of mono- and di-butyl-stannoane complexes. *Inorg. Chim. Acta*, 2017, 455, 627–637.
- Beckmann J., Dakternieks D., Duthie A., Kuan F.S., Tiekkink E.R.T., Synthesis and structures of new oligomethylene-bridged double ladders. How far can layers be separated? *N. J. Chem.*, 2004, 28, 1268–1276.
- Betteridge P.W., Carruthers J.R., Cooper I.R., Prout K., Watkin D.J., “CRYSTALS Version 12: software for guided crystal structure analysis. *J. Appl. Cryst.*, 2003, 36, 1487.
- Cavka J.H., Jakobsen S., Olsbye U., Guillou N., Lamberti C., Bordiga S., et al. A New Zirconium inorganic building brick forming metal organic frameworks with exceptional stability. *J. Am. Chem. Soc.*, 2008, 130, 13850–13851.
- Chandrasekhar V., Gopal K., Sasikumar P., Thirumoorthi R., Organooxotin assemblies from SnC bond cleavage reactions. *Coord. Chem. Rev.*, 2005, 249, 17–18, 1745–1765.
- Chandrasekhar V., Nagendran S., Baskar V., Organotin assemblies containing Sn–O bonds. *Coord. Chem. Rev.*, 2002, 235, 1–52.

- Diop T., Ndoliéne A., Diop M.B., Boye M.S., Lee A.V.D., Dumitru F., et al., Synthesis, spectral (FT-IR, 1H, 13C) studies, and crystal structure of [(2,6-CO<sub>2</sub>)<sub>2</sub>C<sub>5</sub>H<sub>3</sub>NSnBu<sub>2</sub>(H<sub>2</sub>O)]<sub>2</sub>-CHCl<sub>3</sub>. Z. Naturforsch., B: Chem. Sci., 2021, 76, 127–132.
- Dolomanov O.V., Bourhis L.J., Gildea R.J., Howard J.A.K., Puschmann H., OLEX2: A complete structure solution, refinement and analysis Program. J. Appl. Cryst., 2009, 42, 339–341.
- Eng G., Song X., Zapata A., De Dios A.C., Casabianca L., Pike R.D., Synthesis, structural and larvicidal studies of some triorganotin 2-(*p*-chlorophenyl)-3-methylbutyrates. J. Organomet. Chem., 2007, 692, 1398–1404.
- García-Zarracino R., Höpfl H., Rodríguez M.G., Bis(tetraorganodistannoxanes) as secondary building block units (SBUs) for the generation of porous materials – A three-dimensional honeycomb architecture containing adamantane-type water clusters. Cryst. Growth & Des., 2009, 9, 1651–1654.
- Gielen M., Biesemans M., Willem R., Organotin compounds: from kinetics to stereochemistry and antitumour activities. Appl. Organomet. Chem., 2005, 19, 440–450.
- Hanif M., Hussain M., Saqib A., Bhatti M.H., Ahmed M.S., Mirza B., et al., In vitro biological studies and structural elucidation of organotin(IV) derivatives of 6-nitropiperonylic acid: Crystal structure of {[CH<sub>2</sub>O<sub>2</sub>C<sub>6</sub>H<sub>2</sub>(o-NO<sub>2</sub>)COO]SnBu<sub>2</sub>}<sub>2</sub>O}. Polyhedron, 2010, 29, 613–619.
- Kemmer M., Dalil H., Biesemans M., Martins J.C., Mahieu B., Horn E., et al., Dibutyltin perfluoroalkanecarboxylates: synthesis, NMR characterization and in vitro antitumour activity. J. Organomet. Chem., 2000, 608, 63–70.
- Li Q., Wang F., Zhang R., Cui J., Ma C., Syntheses and characterization of organostannoxanes derived from 2-chloroisonicotinic acid: Tetranuclear and hexanuclear. Polyhedron, 2015, 85, 361–368.
- Li W., Du D., Liu S., Zhu C., Sakho A.M., Zhu D., et al., Self-assembly of a novel 2D network polymer: Syntheses, characterization, crystal structure and properties of a four-tin-nuclear 36-membered diorganotin(IV) macrocyclic carboxylate. J. Organomet. Chem., 2010, 695, 2153–2159.
- Ma C., Jiang Q., Zhang R., Synthesis and structure of a novel tri-nuclear 18-membered macrocycle of diphenyltin complexes with 2-mercaptopnicotinic acid. J. Organomet. Chem., 2003, 678, 148–155.
- Macrae C.F., Bruno I.J., Chisholm J.A., Edgington P.R., McCabe P., Pidcock E., et al., Mercury CSD 2.0 – new features for the visualization and investigation of crystal structures J. Appl. Cryst., 2008, 41, 466–470.
- Nakamoto K., Infrared and Raman spectra of inorganic and coordination compounds, 5th ed. New York: John Wiley and Sons, 1997.
- Najafi E., Amini M.M., Khavasi H.R., Weng Ng.S., The effect of substituents of the 1,10-phenanthroline ligand on the nature of diorganotin(IV) complexes formation. J. Organomet. Chem., 2014, 749, 370–378.
- Ng W. S., Monoclinic modification of bis(l2-pyridine-2,6-dicarboxylato)-κ<sup>4</sup>O<sup>2</sup>,N,O<sup>6</sup>:O<sup>6</sup>; κ<sup>4</sup>, O<sup>2</sup>:O<sup>2</sup>,N,O<sup>6</sup> - bis[aquadibutyltin(IV)]. Acta Cryst., 2011, E67, m277.
- Palatinus L., Chapuis G. J., SUPERFLIP – a computer program for the solution of crystal structures by charge flipping in arbitrary dimensions, Appl. Cryst., 2007, 40, 786–790.
- Pruchnik H., Latocha M., Zielinska A., Ułaszewski S., Pruchnik F.P., Butyltin(IV) 5-sulfosalicylates: Structural characterization and their cytostatic activity. Polyhedron, 2013, 49, 223–233.
- Shankar R., Dubey A., Hydrothermal approach for reticular synthesis of coordination assemblies with dicarboxylatotetramethyldistannoxanes as the secondary building units. Eur. J. Inorg. Chem., 2020, 2020, 3877–3883.
- Valcarcel J.A., Razo-Hernandez R.S., Valdez-Velazquez L.L., Garcia M.V., Organillo, A.A.R., Vazquez-Vuelvas O.F., et al., Antitumor structure–activity relationship in bis-stannoxane derivatives from pyridine dicarboxylic and benzoic acids. Inorg. Chim. Acta., 2012, 392, 229–235.
- Vieira F.T., de Lima G.M., Maia J.R. da S., Speziali N.L., Ardisson J.D., et al., Synthesis, characterization and biocidal activity of new organotin complexes of 2-(3-oxocyclohex-1-enyl)benzoic acid. Eur. J. Med. Chem., 2010, 45, 883–889.
- Wang Q.F., Ma C.L., He G.F., Li Z., Synthesis and characterization of new tin derivatives derived from 3,5,6-trichlorosalicylic acid: Cage, chain and ladder X-ray crystal structures. Polyhedron, 2013, 49, 177–182.
- Wang S., Li Q.-L., Zhang R.-F., Du J.-Y., Li Y.-X., Ma C.-L., Novel organotin(IV) complexes derived from 4-carboxybenzenesulfonamide: Synthesis, structure and *in vitro* cytostatic activity evaluation. Polyhedron, 2019, 158, 15–24.
- Watkin D.J., Prout C.K., Pearce L.J., CAMERON, Chemical Crystallography Laboratory, Oxford, UK. 1996.
- Wen G.-H., Zhang R.-F., Li Q.-L., Zhang S.-L., Ru J., Du J.-Y., et al., Synthesis, structure and *in vitro* cytostatic activity study of the novel organotin(IV) derivatives of *p*-aminobenzenesulfonic acid. J. Organomet. Chem., 2018, 861, 151–158.
- Willem R., Bouhdid A., Mahieu B., Ghys L., Biesemans M., Tiekkink E.R.T., et al., Synthesis, characterization and *in vitro* antitumour activity of triphenyl- and *n*-butyltin benzoates, phenylacetates and cinnamates. J. Organomet. Chem., 1997, 531, 151–158.
- Xiao X., Shao K., Yan L., Mei Z., Zhu D., Xu L., A novel macrocyclic organotin carboxylate containing a nona-nuclear long ladder. Dalton Trans. 2013, 42, 15387–15390.
- Zhang R., Zhang S., Ma C., Syntheses, characterization and crystal structures of 1D and 2D organotin polymers containing 3-methyladic acid ligand. J. Inorg. Organomet. Polym., 2012, 22, 500–506.
- Zhu C., Yang L., Li D., Zhang Q., Dou J., Wang D., Synthesis, characterization, crystal structure and antitumor activity of organotin(IV) compounds bearing ferrocenecarboxylic acid. Inorg. Chim. Acta, 2011, 375, 150–157.